Passive TiO_2 growth studies using Medium Energy Ion Scattering and Nuclear Reaction Profiling

M. Brocklebank[1], J.J. Noël[2], L.V. Goncharova[1,2]

mbrockle@uwo.ca

[1]*Department of Physics and Astronomy, Western University, 1151 Richmond St., London, ON, Canada.*
[2]*Chemistry Department, Western University, London, ON, Canada*

Titanium is used pervasively over a range of fields from medical devices and aerospace, to nuclear plants components [1]. Additionally, its oxide is highly valued for its unique surface properties [2] that can be important for a variety of applications. For example, Ti is ubiquitous in biomedical applications as implants, due to its low reactivity with the surrounding tissues. This is due to the surface properties of a naturally forming oxide on Ti [3]. The oxide is stable thermodynamically and few reactions occur on the surface of the implants. However, many factors can impact this process through modifications of its surface energy: composition, structure, roughness and the tissue or fluid environment [4]. For example, electrochemically formed oxide films on Ti can be amorphous or crystalline, depending on the final anodization potential and electrolyte involved [5]. This can directly affect the biocompatibility of Ti, as thickness and crystallinity (rutile vs. anatase) can affect the degree of adsorption from human blood plasma [6]: i.e. rutile has closer packed structure with less ion diffusion compared to anatase. Thus understanding the oxidation at an atomistic level is necessary if you wish to develop better protective films.

Magnetron sputtering was used to deposit Ti onto Si(001). The Ti film was exposed to isotopic ^{18}O water vapour in Ar atmosphere to form an ultra-thin TiO_2 film in situ. The TiO_2/Ti/Si(001) film was then electrochemically oxidized in $D_2{}^{16}O$ water over a range of voltages from 0-10 V, resulting in ~40–295 Å thick oxide regions. In conjunction with this isotopic labeling, medium energy ion scattering (MEIS) and nuclear reaction profiling (NRP) were used to determine the depth profiles of the ^{16}O and ^{18}O in an attempt to elucidate O transport in the TiO_2. Surface composition was determined using X-ray photoelectron spectroscopy and crystallinity was determined using X-ray diffraction.

Fig.1(b) illustrates how the ^{18}O depth distribution changes as a function of voltage. Initially, ^{18}O accounts for 40% of the O in the ~40 Å oxide.

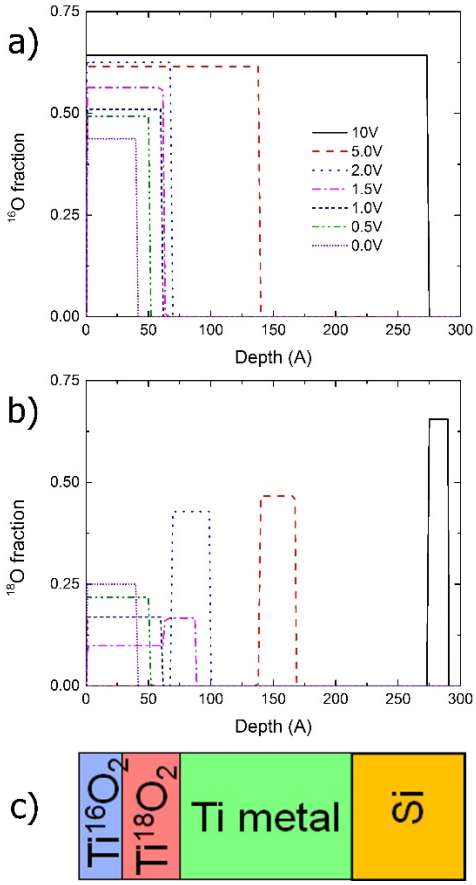

Figure 1: Isotopic depth profiles for (a) ^{16}O and (b) ^{18}O as functions of anodization voltage 0-10 V. These depth profiles are created from simulations of MEIS spectra. Total O concentration for each of these samples is plotted in Figure 2(a). (c) A schematic of the sample involved.

As the anoidization voltage increases, the total concentration of ^{18}O remains constant, which can be seen in Fig.2(b), despite the total oxide thickness increasing monotonically, as seen in Fig.2(a). From to 0.5 V and 1.0 V, the concentration of ^{18}O decreases at the surface and ^{18}O becomes buried deeper. When the voltage reaches 1.5 V, the ^{18}O concentration has decreased at the surface but simultaneously is increasing at greater depths, i.e. new oxide is being created at greater depths. At 2 V, there is no longer any ^{18}O for the first 70 Å of oxide but it accounts for all oxide after that depth, with a stoichiometry $TiO_{0.7}$, which represents a value averaged from oxide and metal phases (i.e. suboxide). From 2 V to 10 V, the depth at which ^{18}O is seen, increases, as does the concentration, but the total amount of the isotope remains constant, confined to an increasingly smaller depth range. At 10 V, all the ^{18}O is confined to a region at 15 Å with a stoichiometry of TiO_2 at a depth of 275 Å into the sample. At this voltage, all the originally sputtered Ti, except for 5 Å (using bulk density), was converted to TiO_2 which is illustrated in Fig.2(b). Thus, oxide forming at deeper depths is due to the transport and incorporation of ^{18}O.

Consistent with the transport of ^{18}O are the depth profiles of ^{16}O, which are presented in Fig.1(b). From Fig.2(a) the ^{18}O concentration can been seen to remain constant, while the ^{16}O concentration rises monotonically as a function of voltage, consistent with the increase in

prevalence of Ti in an oxide phase. Thus increasing incorporation of ^{16}O is the reason for the oxide growth at the oxide-environment interface and given the simultaneously decreasing concentration of ^{18}O, the mechanism for new oxide growth at the oxide-environment interface is through exchange.

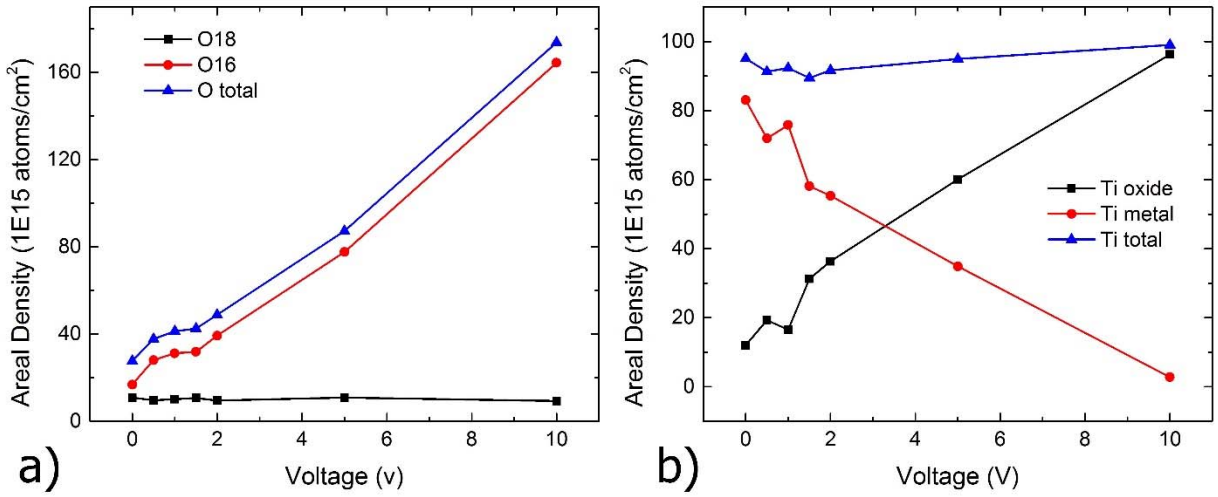

Figure 2: The change in for composition as a function of oxidizing voltage in the anodized Ti: (a) Oxygen exchange curves (b) Total Ti concentration and prevalence of Ti in both the oxide and the metal phases.

Thus, oxide growth increases as function of voltage with increasing incorporation of ^{16}O towards the oxide-environment interface, while ^{18}O is transported to greater depths (while the total amount of ^{18}O remains constant) implying that this occurs via O exchange reactions. Simultaneously new oxide is created by ^{18}O being transported towards the oxide/metal interface, all of which is consistent with O ions as a mobile species but additionally with the possibility Ti ions may be transported towards the oxide-oxidant interface.

References:

[1] The uses of titanium. J.R.B. Gilbert. Mat. Sci. and Tech. 1 (1985) pp 257-262

[2] The surface science of titanium dioxie. U. Diebold. Surface science reports 48 (2003) pp 53-229

[3] Spectroscopic characterization of passivated titanium in a physiologic solution. J.L. Ong, L.C. Lucas, G.N. Raikar, R. Connaster, J.C. Gregory. J. Mater Sci. Mater Med. 6 (1995) pp 113-116

[4] A comparison of the surface characteristics and ion release of Ti6Al4V and heat-treated Ti6Al4V. T.M. Yang, E. Chang, and C.Y. Yang. J. Biomed. Mater Res. 50 (200) pp 499-511

[5] Potentiodynamic behavior of mechanically polished titanium electrodes. O.R. Camara, C.P. Pauli, M.C. Giordano. Electrochimica Acta 29 (1984) pp 1111-1117

[6] Formation and characteristics of the apatite layer on plasma-sprayed hydroxyapatite coatings in simulated body Fluid. J. Weng, Q. Liu, J.G. Wolke, X. Zhang, K. de Groot. Biomaterials 18 (2997) pp 1027-1035